

Acceleration strategies for whole brain quantitative Magnetization Transfer Imaging

Marco Battiston¹, Francesco Grussu^{1,2}, Torben Schneider³, Ferran Prados^{1,4}, Sebastien Ourselin⁴, Claudia A Gandini Wheeler-Kingshott^{1,5,6}, and Rebecca S Samson¹

- (1) Queen Square MS Centre, UCL Institute of Neurology, Faculty of Brain Sciences, University College London, London (UK)
- (2) Centre for Medical Image Computing, Department of Computer Science, University College London, London (UK)
- (3) Philips UK, Surrey, England (UK)
- (4) Translational Imaging Group, Centre for Medical Image Computing (CMIC), Department of Medical Physics and Bioengineering, University College London, London, United Kingdom
- (5) Department of Brain and Behavioural Sciences, University of Pavia, Pavia, Italy
- (6) Brain MRI 3T Research Centre, C. Mondino National Neurological Institute, Pavia, Italy

Synopsis:

Methods for quantitative measurement of myelin are of great interest for understanding brain tissue microstructure, and have potentially important implications in clinical settings for improved diagnosis and prognosis in demyelinating diseases. Quantitative Magnetization Transfer (qMT) has been proposed as a sensitive MRI technique for myelin mapping in the central nervous system. However, after an initial wave of interest, it has never found a successful translation into a clinical scenario, mostly due to its prohibitive scan time. Here we investigate solutions to promote the development of fast qMT protocols including simultaneous multi-slice EPI, and provide preliminary results *in vivo*.

Introduction

Quantitative Magnetization Transfer (qMT) provides a measure of macromolecular tissue content through the bound pool fraction (BPF), suggested as a sensitive myelin biomarker in the brain and spinal cord¹.

Implementation of qMT within clinically accepted times remains challenging. Rapid qMT approaches recently proposed^{2,3} necessarily introduce approximations in the signal modelling and involve constraints on unknown tissue parameters, whose validity needs to be demonstrated on a case-specific basis⁴.

Here, we investigate alternative methodologies to perform and speed up qMT acquisition *in vivo*. In particular, (i) qMT is implemented by means of an EPI readout to allow a high number of data points to be acquired, (ii) a more general model fitting approach is considered, removing the necessity for separate measurement of the longitudinal relaxation time (T_1^{obs}), and (iii) Simultaneous-multi-slice (SMS) excitation is used to accelerate acquisition.

Methods

MT-weighted (MT-w) volumes are acquired using off-resonance pulse trains followed by spin-echo single-shot EPI readouts of slice packages (each including 12 slices), with the following sequence parameters: 48 2.5mm thick slices, resolution $2.25 \times 2.25 \text{mm}^2$, in-plane SENSE factor=2, TE=34ms, 30 MT pulses per train with 15ms duration and 5ms gap, TR=7700ms; acquisition time 35s for each MT-w volume.

24 MT-w volumes (with varying pulse amplitude and offset frequency, selected following protocol optimization as in⁵) and 12 M_0 (unsaturated) volumes (for signal normalization) are acquired in 19:30minutes.

We fit the two-pool model to the data⁶ to estimate BPF, free and bound water T_2 (T_2^{F} and T_2^{B}) and free-to-bound water exchange (k_{FB}), following T_1^{obs} quantification from an Inversion Recovery (IR) protocol with the same EPI readout, with 12 inversion times (total acquisition time 8:30min).

MT-w and IR data are also acquired with SMS excitation (acceleration factor=2), halving the scan-time for each protocol (09:45min for SMS-MT; 4:30min for SMS-IR).

MT-w data (with and without SMS) are inherently T_1 -weighted. This fact is exploited to directly measure T_1^{obs} without using additional IR data. To enhance T_1 -weighting, slice order is shuffled across sequence repetitions. This mechanism is replicated for M_0 volumes to produce the same inter-slice MT-weighting (due to 2D spin-echo), which has been shown to provide robust correction for such unwanted effects via simple image normalization^{5,7}.

We fit numerical solutions of the two-pool equations⁸ to MT-w datasets, both with and without external T_1^{obs} measurement (4- and 5-parameter fits respectively).

Data from a single subject (male, 29) acquired and analysed with the above pipeline are presented here.

Results

Figure 1 shows qMT model parameters and T_1^{obs} estimated with the EPI-based protocol. Parameters are in the expected range for brain tissue^{9,10}, with BPF and k_{FB} depicting well defined contrast between different tissues, as shown by relative parameter distributions.

T_1^{obs} is estimated using MT-w data in a 5-parameter fit, via the relaxation rate R_1^{F} . Results are shown in figure 2 and compared with the more standard 4-parameter fit. Negligible parameter measurement bias is noticed for T_2^{B} and BPF (inter-quartiles ranges of error distributions are -10.1%;-0.7% and 0.3%;2.5% respectively) , however more pronounced differences are visible for k_{FB} and R_1^{F} (inter-quartiles ranges are -16.4%;-1% and -25.2%;-2.3%) .

Figure 3 compares maps obtained with and without SMS acceleration. T_1^{obs} and T_2^{B} estimates are remarkably similar between the two protocols (numbers?). BPF and k_{FB} show patterns of overestimation and underestimation for short and long BPF/ k_{FB} respectively, captured also by distribution comparison. Overall contrast between tissue types appears preserved.

Figure 4 shows the effect of acceleration strategies on BPF estimates. Acquisition time for BPF estimation can be reduced to 10 minutes at a cost of more noisy estimates, in particular in the presence of partial volume effects with CSF.

Conclusions

We have provided preliminary results in the development of a whole-brain qMT protocol using EPI readout, a solution that remains unexplored as yet¹⁰, despite its potential for multi-contrast brain microstructure examinations¹¹.

Acceleration strategies can be readily incorporated in the proposed protocol: (i) the non-steady-state nature of the acquisition allows the estimation of saturation and relaxation parameters simultaneously; (ii) the incorporation of SMS imaging allows for additional acceleration. Qualitatively, such strategies appear to have limited impact on BPF estimation, which is often the main qMT parameter of interest as it is thought to be sensitive to myelin content.

Further validation and investigation of these initial findings is warranted in order to elucidate the origin of the discrepancies on R_1^{F} between the 4- and 5-parameter fit and to better characterise the MT effect associated with SMS excitation. A correct formulation of such an effect would potentially enable the use of acceleration factors higher than 2, leading to even more effective scan time reductions.

Acknowledgements

UK MS Society. International Spinal Research Trust, Wings for Life and Craig H. Nielsen Foundation (INSPIRED). EPSRC (M020533; through CMIC Pump-Priming Awards). Horizon2020-EU.3.1 (ref: 634541). FP is a Guarantors of Brain non-clinical Fellow

References

- [1] Odrobina E, et al. NMR Biomed 2005, 18:277-284
- [2] Yarnykh V L. MRM 2012, 68:166-178
- [3] Smith A K, et al. Neuroimage 2014, 95:106-116
- [4] Smith A K, et al. NeuroImage clinical 2017, 16:58-65
- [5] Battiston M, et al. MRM 2017, doi:10.1002/mrm.26909

- [6] Henkelmann R M, et al. *MRM* 1993, 29:759-766
- [7] Gelderen P, et al. *MRM* 2017, 77:2174-2185
- [8] Portnoy S, et al. *MRM* 2007, 58:144-155
- [9] Underhill H R, et al. *Neuroimage* 2009, 47:1568-1578
- [10] Yarnykh V L, et al. *Neuroimage* 2004, 23:409-424
- [11] Tyler D J, et al. *MRM* 2005, 53:103-109
- [12] Campbell J SW, et al. *Neuroimage* 2017, doi:10.1016/j.neuroimage.2017.08.038

Figure 1:

qMT parameter maps and T_1^{obs} maps obtained from the MT-EPI protocol and IR-EPI protocol developed in this study (an example slice is shown). qMT parameters are obtained with a 4-parameter fit after quantification of T_1^{obs} from a separate acquisition. Relative distributions of each parameter over the whole brain are shown in the bottom panels.

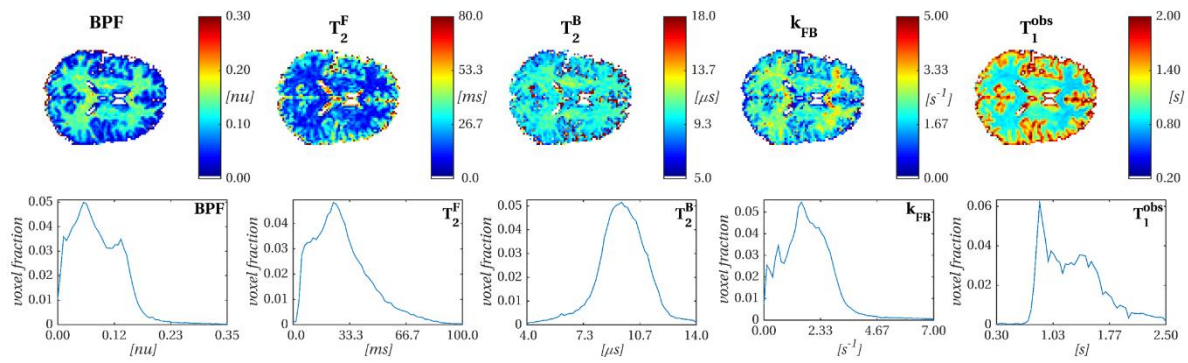


Figure 2:

Comparison between fitting approaches on MT-w data acquired with the proposed EPI-based protocol. Results from an example slice are shown for the 4-parameter fit (first row) and the 5-parameter fit (second row). Bottom panels (red box) refer to relative errors between fitting approaches calculated voxel-wise as $(4\text{par}-5\text{par})/4\text{par}$. Negative values in the difference maps mean overestimation in the 5-parameter fit approach. To ease the comparison, T_1^{obs} obtained from IR data in the 4-parameter fit is converted into R_1^{F} once qMT model parameters are determined.

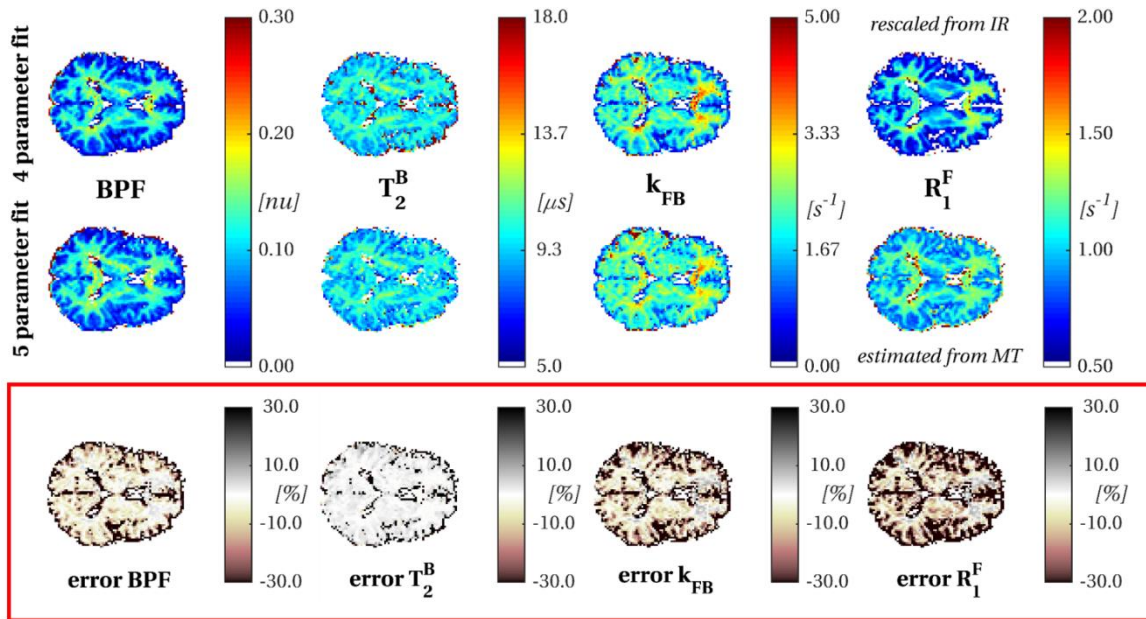


Figure 3

Comparison between qMT model parameters estimated from MT-w data acquired without (top row) and with (second row) SMS imaging. Results are shown for the 4-parameter fit approach in an example slice. To ease evaluation of differences in the quantitative maps, distributions of qMT parameters are also shown for standard EPI (blue) and SMS-EPI (orange) acquisition.

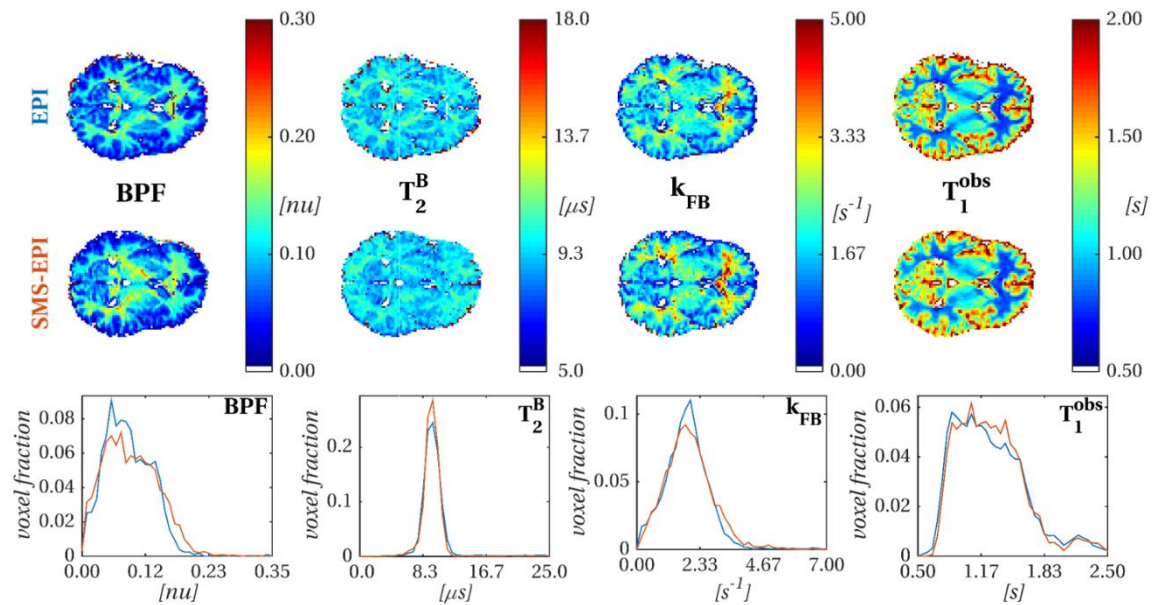


Figure 4

Effect of the various acceleration strategies investigated in this work on the BPF map, for an example slice. From left to right: MT-w data with standard EPI and 4-parameter fit, MT-w data with standard EPI and 5-parameter fit, MT-w data with SMS-EPI and 4-parameter fit, MT-w data with SMS-EPI and 5-parameter fit. For each case, the scan time required is reported at the bottom.

